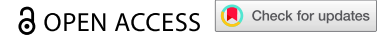


RESEARCH ARTICLE



Antenatal *Ureaplasma* infection induces ovine small intestinal goblet cell defects: a strong link with NEC pathology

Charlotte van Gorp^a, Ilse H de Lange^{a,b,c}, Matthias C Hütten^{a,d}, Carmen López-Iglesias^e, Kimberly RI Massy^a, Lilian Kessels^a, Boris Kramer^a, Willine van de Wetering^e, Brad Spiller^f, George M Birchenough^{g,h}, Wim G van Gemert^{b,c}, Luc J Zimmermann^a, and Tim GAM Wolfs^{a,i}

^aDepartment of Pediatrics, School of Oncology and Reproduction (GROW), Maastricht University, Maastricht, The Netherlands; ^bDepartment of Surgery, School for Nutrition, Toxicology and Metabolism (NUTRIM), Maastricht University, Maastricht, The Netherlands; ^cEuropean Surgical Center Aachen-Maastricht, Department of Pediatric Surgery, School for Nutrition, Toxicology and Metabolism (NUTRIM), Maastricht University, Maastricht, The Netherlands; ^dNeonatology, Department of Pediatrics, Maastricht University Medical Center, Maastricht, The Netherlands; ^eMicroscopy CORE Lab, Maastricht Multimodal Molecular Imaging Institute (M4I), Maastricht University, Maastricht, The Netherlands; ^fDivision of Infection and Immunity, School of Medicine, Cardiff University, Cardiff, UK; ^gDepartment of Medical Biochemistry, Institute of Biomedicine, University of Gothenburg, Gothenburg, Sweden; ^hWallenberg Center for Molecular and Translational Medicine, University of Gothenburg, Gothenburg, Sweden; ⁱDepartment of Biomedical Engineering (BMT), School for Cardiovascular Diseases (CARIM), Maastricht University, Maastricht, The Netherlands

ABSTRACT

Disruption of the intestinal mucus barrier and intestinal epithelial endoplasmic reticulum (ER) stress contribute to necrotizing enterocolitis (NEC). Previously, we observed intestinal goblet cell loss and increased intestinal epithelial ER stress following chorioamnionitis. Here, we investigated how chorioamnionitis affects goblet cells by assessing their cellular characteristics. Importantly, goblet cell features are compared with those in clinical NEC biopsies. Mucus thickness was assessed as read-out of goblet cell function. Fetal lambs were intra-amniotically (IA) infected for 7d at 122 gestational age with *Ureaplasma parvum* serovar-3, the main microorganism clinically associated with chorioamnionitis. After preterm delivery, mucus thickness, goblet cell numbers, gut inflammation, epithelial proliferation and apoptosis and intestinal epithelial ER stress were investigated in the terminal ileum. Next, goblet cell morphological alterations (TEM) were studied and compared to human NEC samples. Ileal mucus thickness and goblet cell numbers were elevated following IA UP exposure. Increased pro-apoptotic ER stress, detected by elevated CHOP-positive cell counts and disrupted organelle morphology of secretory cells in the intestinal epithelium, was observed in IA UP exposed animals. Importantly, comparable cellular morphological alterations were observed in the ileum from NEC patients. In conclusion, UP-driven chorioamnionitis leads to a thickened ileal mucus layer and mucus hypersecretion from goblet cells. Since this was associated with pro-apoptotic ER stress and organelle disruption, mucus barrier alterations seem to occur at the expense of goblet cell resilience and may therefore predispose to detrimental intestinal outcomes. The remarkable overlap of these *in utero* findings with observations in NEC patients underscores their clinical relevance.

ARTICLE HISTORY

Received 31 May 2022
Revised 05 December 2022
Accepted 05 Dec 2022



KEYWORDS

Chorioamnionitis; NEC; TEM; mucus; ER stress; goblet cell


Introduction

Ureaplasma parvum (UP) is frequently isolated from the amniotic fluid (AF) and uterine membranes of women with chorioamnionitis.¹ Chorioamnionitis is characterized by an inflammatory cell influx into fetal membranes and is an important cause of preterm birth.² Although chorioamnionitis is often clinically silent, it can affect the fetus through direct contact with the contaminated amniotic fluid³ and via systemic

inflammation in the fetus called fetal inflammatory response syndrome (FIRS). We have previously shown, in an ovine chorioamnionitis model, that UP-induced chorioamnionitis caused intestinal inflammation, injury and developmental disruptions.^{4,5} Consequently, chorioamnionitis and FIRS are associated with increased neonatal morbidity and mortality^{6,7} including necrotizing enterocolitis (NEC).⁸ NEC is a severe gut disease that mainly affects premature neonates.⁹ It is

CONTACT Tim GAM Wolfs  tim.wolfs@maastrichtuniversity.nl  Department of Pediatrics, School of Oncology and Reproduction (GROW), Maastricht University, Universiteitssingel 50, 6202 ER Maastricht, The Netherlands

This article has been republished with minor changes. These changes do not impact the academic content of the article.

 Supplemental data for this article can be accessed online at <https://doi.org/10.1080/21688370.2022.2158016>

© 2022 The Author(s). Published with license by Taylor & Francis Group, LLC.

This is an Open Access article distributed under the terms of the Creative Commons Attribution-NonCommercial-NoDerivatives License (<http://creativecommons.org/licenses/by-nc-nd/4.0/>), which permits non-commercial re-use, distribution, and reproduction in any medium, provided the original work is properly cited, and is not altered, transformed, or built upon in any way. The terms on which this article has been published allow the posting of the Accepted Manuscript in a repository by the author(s) or with their consent.

characterized by intestinal inflammation and, in progressing disease, gut necrosis. Mortality generally ranges from 20% to 30% and survivors are at risk of long-term morbidities including short-bowel syndrome and neurodevelopmental delays.⁹

Despite being an important research topic in neonatology for years, NEC pathophysiology is still incompletely understood. One previously described contributing factor is disruption of the intestinal mucus barrier with goblet cell loss and reduced mucin production.^{10–12} In a healthy gut, a mucus layer, formed by gel-forming mucins that are secreted by goblet cells, separates the intestinal epithelium from the gut lumen and prevents bacteria from adhering to the epithelial surface.¹⁰ Upon disruption, bacteria reach the intestinal epithelial cells and trigger inflammation.¹⁰ In previous preclinical chorioamnionitis studies using lipopolysaccharides (LPS) as inflammatory stimulus, it was observed that chorioamnionitis induces *in utero* goblet cell loss, suggesting mucus barrier alterations may, at least in part, form a mechanistic explanation for the association between chorioamnionitis and NEC.^{13,14} Additionally, goblet cell loss was found to be associated with intestinal inflammation, intestinal epithelial endoplasmic reticulum (ER) stress and apoptosis.¹⁴ These combined findings suggest that impaired development of mature goblet cells by ER-stress driven apoptosis was mechanistically involved.¹⁴ Importantly, ER stress is causally linked with the pathophysiology of several intestinal diseases, including inflammatory bowel disease¹⁵ and NEC.^{16,17} A key function of the ER is the folding of proteins following ribosomal protein synthesis. If the ER's capacity to fold proteins is exceeded, ER stress occurs and the unfolded protein response (UPR) will be initiated by binding immunoglobulin protein (BiP) to support ER stress resolution.^{18,19} Once the UPR is unable to resolve ER stress, apoptosis will be induced through, amongst other mechanisms, upregulation of transcription factor C/enhancer binding protein homologous protein (CHOP).²⁰

Here, we investigated how goblet cells are affected following UP-induced chorioamnionitis by examining cellular mechanisms including studying goblet cell counts, intestinal epithelial apoptosis and intestinal epithelial ER stress and by in-depth analysis of

goblet cell characteristics in the terminal ileum with transmission electron microscopy (TEM). Moreover, we studied the thickness of the ileal mucus layer as read-out for goblet cell function. Importantly, we compared morphological goblet cell alterations during chorioamnionitis with those in clinical ileal NEC biopsies and gestation matched controls.

Material and methods

Experimental design

Animal experiments were approved by the animal experimentation committee of Maastricht University (registration number PV2015–005–02). The ovine model used and experimental procedures have been described in detail previously.^{5,21} The study design is presented in Supplementary figure 1. Ten time-mated Texel ewes carrying twin fetuses were randomly assigned (per twin) to two groups of eight to ten animals. One lamb was appointed to a different experiment and one lamb was excluded because of a humane endpoint. At 122d gestational age (GA), ewes (both amniotic sacs) were intra-amniotically (IA) injected with viable *Ureaplasma parvum* serovar-3 (HPA5 strain, 10⁷ color changing units (CCU)) or saline (controls). Fetuses were delivered preterm via cesarean section at 129d GA (term ~150d GA), equivalent to approximately 30–32 weeks of human gastrointestinal development, and subsequently euthanized. Euthanasia and tissue sampling procedures are described in Supplementary file 1.

Alcian Blue/Periodic Acid Schiff (AB-PAS)

AB-PAS was used as marker for mature (e.g., glycosylated) mucins^{22,23} Staining was performed on 4 µm thick paraffin embedded Carnoy's solution fixated terminal ileum sections as previously described,¹⁴ with the exception of a shorter incubation with Alcian blue of 15 minutes in the current study.

Immunohistochemistry

For immunohistochemical stainings, 4 µm thick paraffin embedded paraformaldehyde fixated (Ki67, CC3, CHOP, IBA1 and BiP) or Carnoy's solution fixated (MUC2) terminal ileum sections were used. Staining procedures were described

previously²¹ and are summarized in Supplementary file 2. Antibodies used are listed in Supplementary table 1.

Analysis of stained sections (AB-PAS and immunohistochemistry)

Stained sections were scanned using Ventana iScan (Ventana Medical System, Inc., Tucson, AZ). Cells that were positively stained for AB-PAS, CC3, CHOP, Ki67 and MUC2 were counted in a semi-automated fashion with the use of QuPath quantitative pathology and bioimage analysis software version 0.20 (University of Edinburgh, Edinburgh, UK).²⁴ For AB-PAS, BiP and MUC2, lower villus, middle villus and villus tips were analyzed separately as previously described¹⁴ to investigate regional differences. For BiP and CHOP, crypts were analyzed separately. Crypts were not analyzed for AB-PAS and MUC2, since these markers are expressed by both goblet cells and Paneth cells. Mucosal surface area and IBA1 positively stained surface area (macrophages) were measured in Leica QWin Pro version 3.4.0 (Leica Microsystems). Positive cell count and positively stained surface area were corrected for mucosal surface area and presented as positive cell count per mm² ileal surface area or percentage of positively stained ileal surface area. Quantitative analyses were performed by one investigator blinded to the experimental groups. Qualitative assessment of BiP staining intensity was assessed by two independent blinded researchers. The scoring system used was previously reported,¹⁴ 0: no staining, 1: mild staining, 2: moderate staining, 3: intense staining.

RNA isolation, cDNA synthesis and RT-qPCR

Snap frozen terminal ileum was lysed and homogenized and RNA was isolated with the RNeasy Mini Kit (#74104, Qiagen, Hilden, Germany). cDNA was synthesized with the SensiFast cDNA synthesis kit (BIO-65054, Bioline, London, UK). Real-time (RT) qPCR was performed with the SensiMix SYBR Hi-Rox kit (QT605-05, Bioline) and LightCycler-580 Instrument (Roche Applied Science, Basel, Switzerland). Ovine specific primers were used (Supplementary table 2). RT-qPCR data processing was performed with LinRegPCR

software (version 2016.0, Heart Failure Research Center, Academic Medical Center, Amsterdam, the Netherlands). The geometric mean of three housekeeping genes (ovRPS15, GAPDH and YWHAZ) was used for data normalization. Delta CT values were used for statistical analyses. Data are presented as fold change compared controls (calculated from delta-delta CT values).

Mucus thickness measurements

After sacrifice, fresh ileal tissue was stored in ice-cold Krebs buffer (NaHCO₃ 24.9 mM, KH₂PO₄ 1.2 mM, MgSO₄ · 7H₂O 1.1 mM, KCl 4.7 mM, NaCl 118.2 mM and CaCl₂·2H₂O 2.5 mM) and kept at 4°C until measurement of mucus thickness within 3 hours after sample collection. Ileal mucus thickness measurements were based on a method developed at the University of Gothenburg, Sweden²⁵ and are described in detail in Supplementary file 3 and Supplementary figure 2.

Human intestinal sample collection

We collected gut samples and clinical data of five pediatric patients undergoing ileal resection for acute NEC (patient 1–3), stoma reversal after NEC (patient 4) and stoma reversal after meconium ileus (patient 5). Patients were born prematurely and were treated at the neonatal intensive care unit during surgery. The study was approved by the Medical Ethical Committee of Maastricht University Medical Center (registration number 16–5–185). All parents gave written informed consent. After tissue removal, ileum was kept on ice and fixated in Karnovsky's fixative for TEM analysis.

Transmission electron microscopy (TEM)

For TEM, ileum samples from randomly selected fetal lambs (N = 5 controls and N = 6 UP exposed lambs), human NEC (N = 3) and human control tissue (N = 2) were prepared for imaging as described in Supplementary file 1. Following tissue processing and cutting, ultrathin sections were mounted on Formvar-coated copper grids and stained with 2% uranyl acetate in 50% ethanol and lead citrate. We imaged stained sections of all EM

fixed ileal samples using a Tecnai G2 Spirit transmission electron microscope with a CCD Eagle 4kx4k camera (Thermo Fisher Scientific).

Statistics

We used GraphPad Prism Software (v6.0, GraphPad software Inc., La Jolla, CA, USA) for statistical analyses. We tested for statistical significance between the groups with a Mann-Whitney U test. Differences were regarded as statistically significant at $p < .05$. Data are displayed as median with interquartile range (IQR) for all outcome measures.

A composite z-score was calculated for the three intestinal inflammatory read-outs (IBA1, TNF α and TGF β). Since the number of animals per group is relatively small, p-values between 0.05 and 0.10 were reported in exact numbers and are regarded as potentially biologically relevant as described previously.^{14,21,26}

Results

Mucus layer thickness in distal ileum of premature lambs

To assess the consequences of IA UP exposure for the small intestinal mucus layer, as read-out for goblet cell function, distal ileal mucus thickness was measured. Ileal mucus thickness was increased in animals IA exposed to UP for 7d compared to controls ($p < 0.05$) (Figure 1a). No differences in villus length were observed between groups (Supplementary figure 3), suggesting the mucus layer thickness was also increased relative to villus length following IA UP exposure.

Presence of goblet cells expressing mature mucins and their distribution in distal ileum of premature lambs

AB-PAS- and MUC2-positive cells were identified in the distal ileum to assess alterations in goblet cell numbers and their expression of the major intestinal gel-forming mucin, since such goblet cell changes could contribute to the increased mucus layer thickness. Compared to controls (Figure 1b), the number of AB-PAS-positive cells was increased

in the lower villus (Figure 1c, d), middle villus (Figure 1c, e) and total villus (Figure 1c, f) of IA UP exposed animals (all $p < 0.05$). In the upper villus region, AB-PAS-positive cell counts did not differ between groups (Supplementary figure 4). The number of MUC2-positive cells did not differ between groups in all regions analyzed (Supplementary figure 5). Collectively, these findings suggest that the number of goblet cells (AB-PAS-positive cells) was increased following IA UP exposure. However, this increase was not linked to additional MUC2-positive cells, indicating the increased numbers of goblet cells might reflect cells producing alternative gel-forming mucins.²⁷

Signs of mild inflammation in the distal ileum of premature lambs

Intestinal inflammation was investigated as potential mechanism underlying the observed increased mucus layer thickness and goblet cell alterations. After 7d of IA UP exposure, 7 out of 8 UP exposed animals had a IBA1 positive surface area (macrophages) above median control level (Figure 2a, b, c), versus 5 out of 10 control animals (Figure 2a, c) and the median percentage IBA1-positive surface area was 1.2% higher following UP exposure (74% relative difference). Regarding TNF α mRNA expression, 6 out of 8 UP exposed animals had delta CT values below median control delta CT values with a difference in median expression of 1.65 CT value (~214% relative levels of mRNA expression) (Figure 2d), and for TGF β mRNA expression 5 out of 8 UP exposed animals had delta CT levels below median control values (Figure 2e) with a difference in median expression of 0.95 CT value (~93% relative levels of mRNA expression). The composite z-score of the three intestinal inflammatory data sets (IBA1, TNF α and TGF β) tended to be increased ($p = 0.10$) following IA UP exposure for 7d compared to control animals (figure 2f).

Collectively, these data indicate mild inflammation of the terminal ileum after 7d of IA UP exposure.

ER-stress and intestinal epithelial apoptosis and proliferation in distal ileum of premature lambs

Intestinal epithelial levels of ER stress were investigated because increased mucus layer thickness

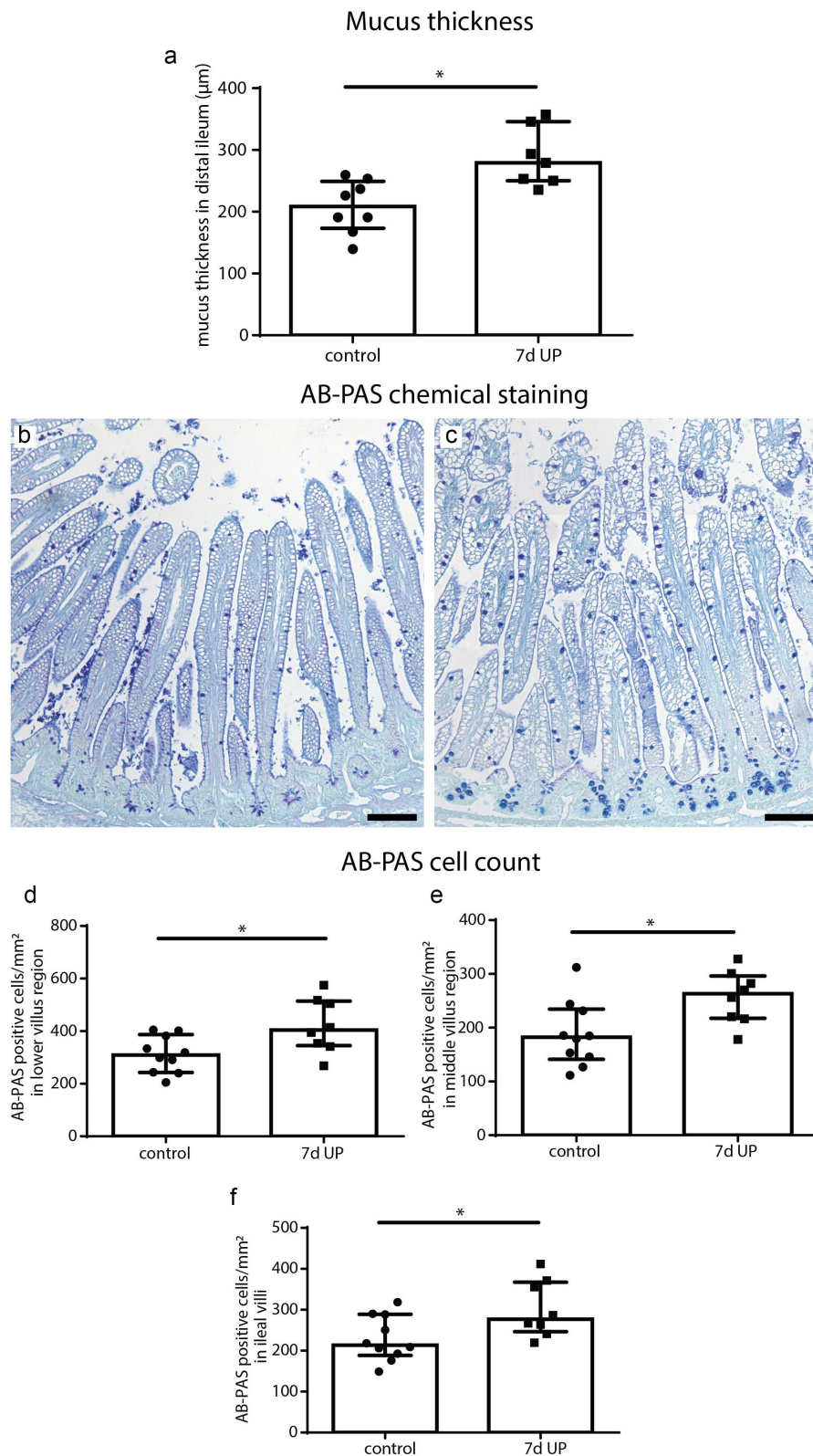


Figure 1. Mucus layer thickness and the number of AB-PAS-positive cells per mm^2 surface area in distal ileum of premature lambs. Compared to control lambs, mucus layer thickness was increased in 7d UP exposed animals (a). Compared to control lambs (b), the number of AB-PAS positive cells was increased in UP exposed lambs (c) in the lower villus region (d), middle villus region (e) and in the total villi (f). Each data point represents the mucus layer thickness or average cell count of one lamb. Data are displayed as median with interquartile range. Scale bar indicates $100 \mu\text{m}$. $*p < 0.05$. Abbreviations: AB-PAS: alcian blue/periodic acid Schiff, IA: intra-amniotic, UP: *Ureaplasma parvum*.

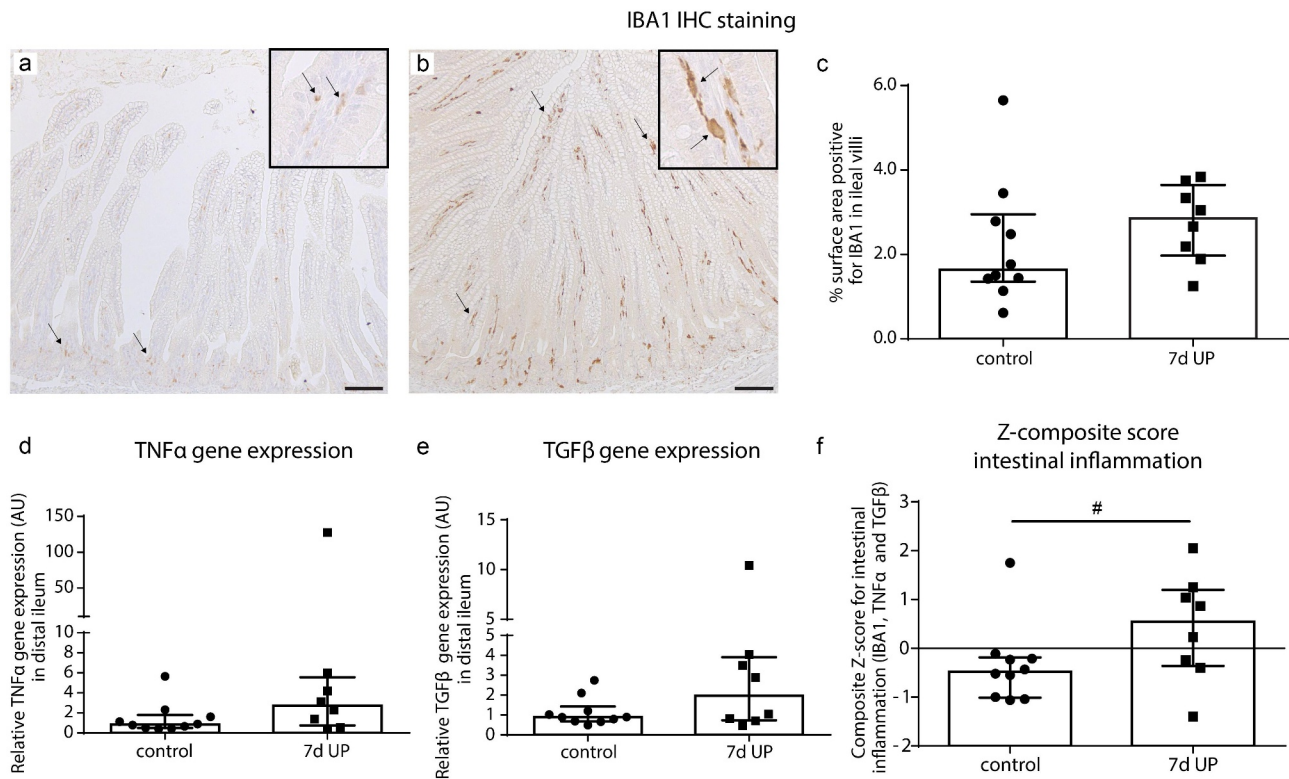


Figure 2. Mild inflammation in the ileum of premature lambs. Mild inflammation was detected in IA UP exposed animals compared to controls, although none of the comparisons reached statistical significance. A mild increase in IBA1 positive surface area (macrophages) (black arrows) (**A, B, C**), TNF α mRNA expression (**d**) and TGF β mRNA expression (**e**) was detected in the ileum of IA UP exposed lambs compared to controls. (**f**) The composite z-score of the intestinal inflammatory data sets (IBA1, TNF α and TGF β) tended to be increased ($p = 0.10$) following 7d IA UP exposure compared to controls. Each data point represents the average positive surface area or relative mRNA expression of one lamb. Data are displayed as median with interquartile range. Scale bar indicates 100 μm . # $0.05 < p \leq 0.10$. Abbreviations: IA: intra-amniotic, IBA1: ionized calcium-binding adaptor molecule 1, TNF α : tumor necrosis factor α , TGF β : transforming growth factor β , UP: *Ureaplasma parvum*.

could result from enhanced mucus secretion by goblet cells, which could induce ER stress. Expression levels of BiP, an important initiator of the UPR to resolve ER stress,^{18,19} were in both groups highest in the lower villus region, but did not differ between controls (**Figure 3a, c**) and IA UP exposed animals (**Figure 3b, c**). In contrast, the number of cells positive for CHOP, a driver of ER-stress induced apoptosis,²⁰ was increased ($p < 0.01$) in ileal crypts (**Figure 3e, f**) and ileal villi (**Figure 3e, g**) of IA UP exposed lambs compared to controls (**Figure 3d, f, g**).

Subsequently, we studied whether the observed ER stress was associated with increased intestinal epithelial apoptosis and whether intestinal epithelial proliferation was altered. Compared to controls (**Figure 3g, j**), the number of apoptotic cells (CC3-positive cell count) was not statistically significantly

altered in IA UP exposed animals (**Figure 3h, i, j**). Apoptosis was primarily detected in the intestinal crypts (**Figure 3g, h**). Of note, two IA UP exposed animals had high amounts of apoptotic cells and in these animals, apoptosis was mainly detected in the lower villus region (**Figure 3i**). No differences in intestinal epithelial proliferation (Ki67-positive cell counts) were detected (Supplementary figure 6).

Thus, 7d of IA UP exposure was associated with pro-apoptotic ER stress and potential increased apoptosis at a later time point.

Cellular morphological alterations in distal ileum of premature lambs – TEM

We performed TEM to investigate whether the elevated epithelial ER stress levels were associated with cellular morphological alterations in the fetal

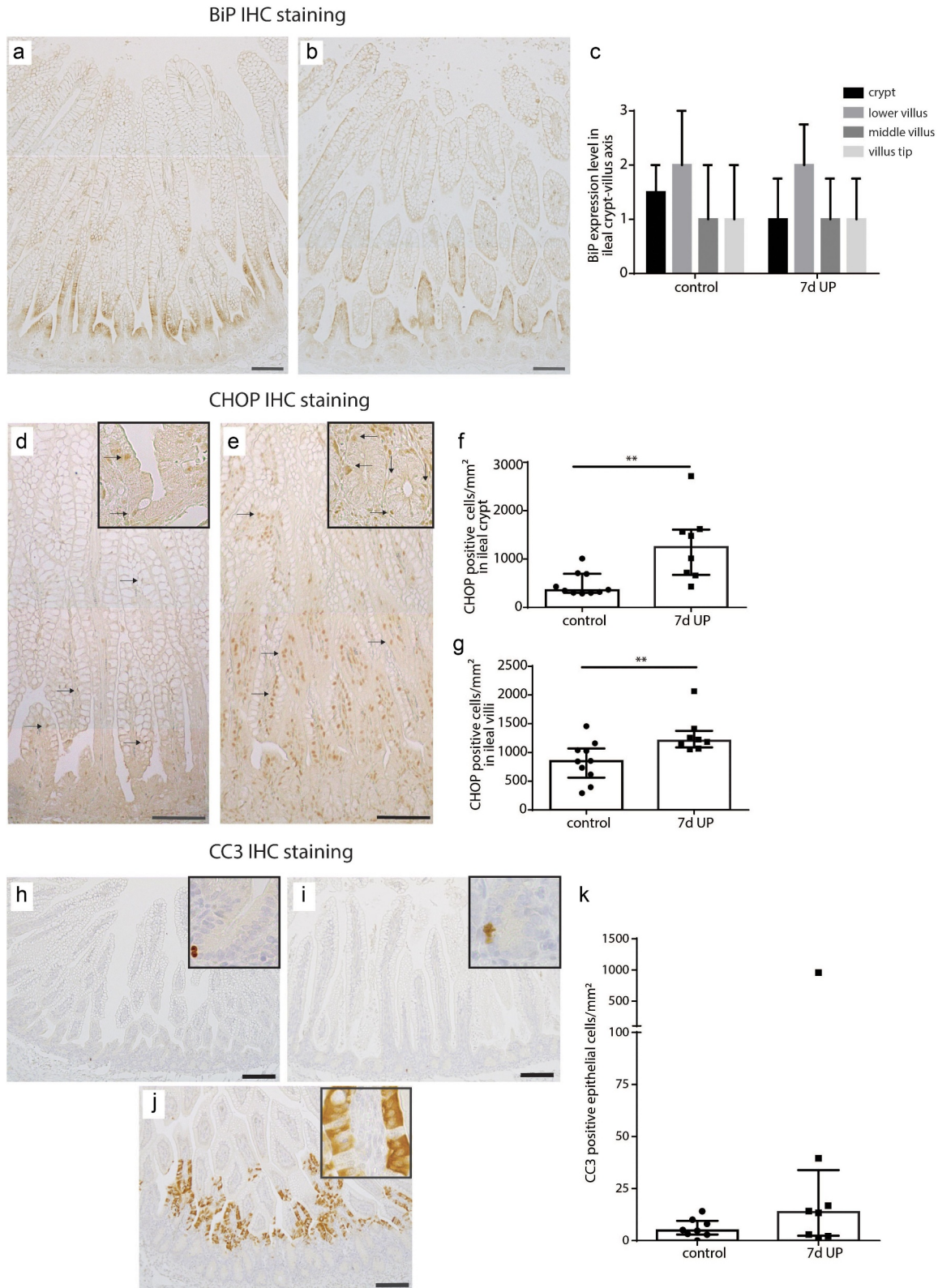


Figure 3. BiP expression pattern along crypt-villus axis, the number of CHOP-positive cells per mm² surface area and the number of CC3-positive cells per mm² surface area in distal ileum of premature lambs. The BiP expression pattern of controls (a, c) was comparable to that of IA UP exposed lambs (b, c). Compared to controls (**D, F, G**), CHOP positive cell count was increased after 7d UP exposure in ileal crypts (e, f) and ileal villi (e, g). The CC3-positive cell count was not statistically significantly different between control (h, j) and IA UP exposed animals (**I, J, K**). However, two IA UP exposed animals had high CC3-positive cell counts and these cells were detected in the lower villus region (j, k). Each dot point represents the average CHOP- or CC3-positive cell count of one lamb. Data are displayed as median with interquartile range. Scale bar indicates 100 μ m. ** $p < 0.01$. Abbreviations: IA: intra-amniotic, BiP: binding immunoglobulin protein, CC3: cleaved caspase 3, CHOP: C/enhancer binding protein homologous protein, IA: intra-amniotic, UP: *Ureaplasma parvum*.

ileum. Interestingly, most pronounced differences were observed in secretory cell types (goblet cells and Paneth cells) in the crypt to villus transition region. In UP exposed animals, in ~60% of the crypts-villus axes in this region affected secretory cells were present, whereas secretory cells of control animals and non-secretory cells in both groups (data not shown) were seldomly altered. In secretory cells of control animals, the mitochondria show an elongated morphology with abundant parallel cristae perpendicular to the mitochondria membrane (Figure 4a), while mitochondria in affected secretory cells in IA UP exposed animals are globular shaped, contain less electron dense matrix and have altered cristae morphology and organization (Figure 4b). The rough endoplasmic reticulum (RER) cisternae show a wide range of sizes and shapes in control animals, from almost parallel membranes with thin spaces in between (Figure 4c) to ovoidal shapes with wider intramembrane spaces (Figure 4a), which are both considered structurally normal. In contrast, in the secretory cells of IA UP exposed animals, the RER does not have recognizable cisternae, but contains big spaces filling the cytoplasm (Figure 4d). Regarding the Golgi apparatus, the differences between control and IA UP exposed animals concern to the dimensions of the saccules, which are clearly swollen in UP exposed animals (Figure 4e, f). Thus, whereas mitochondria, RER and Golgi apparatus are structurally normal in control animals, these organelles are morphologically disrupted in the secretory cells in the transition region from crypt to villus of IA UP exposed animals. In addition, in this region, cells with necrotic characteristics were exclusively detected in the lumen of IA UP exposed animals (Figure 4g, h). In the base of the crypts, no morphological alterations of secretory cell types, including Paneth cells (Supplementary figure 7), were detected.

Morphological differences at cellular level were also observed in the villus region (Figure 5). At organelle level, mitochondria and RER were structurally normal in enterocytes of control animals

with organelle morphologies similar to those observed in the transition region from crypt to villus (Figure 5a, c), whereas these organelles were morphologically disrupted in epithelial cells of ~60% of the villi of IA UP exposed animals (Figure 5b, d). In addition, in small intestinal enterocytes of control animals, small vacuoles were found (Figure 5e), which corresponds to the intestinal cell morphology of fetal enterocytes.²⁸ Remarkably, larger vacuoles were observed in enterocytes of UP exposed animals (figure 5f). Secretory cells were structurally normal in the villus region of both the control group and in UP exposed animals (data not shown).

Collectively, 7d of IA UP exposure was associated with overt cellular morphological alterations of secretory cells in the transition region from crypt to villus and of enterocytes in the villus region.

Cellular morphological alterations in distal ileum of NEC patients and controls – TEM

To investigate whether cellular changes comparable to those observed in UP exposed animals are present in the ileum of NEC patients, TEM was performed on ileal samples of NEC patients and gestation matched controls. Consistent with our findings in IA UP exposed animals, mitochondria, RER and Golgi apparatus were morphologically disrupted in the transition region from crypt to villus in the ileum of NEC patients (Figure 6b, d, f) compared to controls (Figure 6a, c, e). However, in NEC patients, changes were observed in all cell types, the cellular morphological alterations were present in all crypt-villus axes and extended to the whole crypt (compared to crypt to villus transition region in UP exposed animals). In addition, the organization of the crypt region was completely disrupted in most ileal crypts, with presence of a large amount of necrotic cells (Figure 6h), compared to controls (Figure 6g). Interestingly, in crypts that were not fully disrupted, the number of Paneth cells was reduced and Paneth cell granule intensity was diminished in the base of the crypts of NEC patients compared to control ileal samples (Supplementary figure 6).

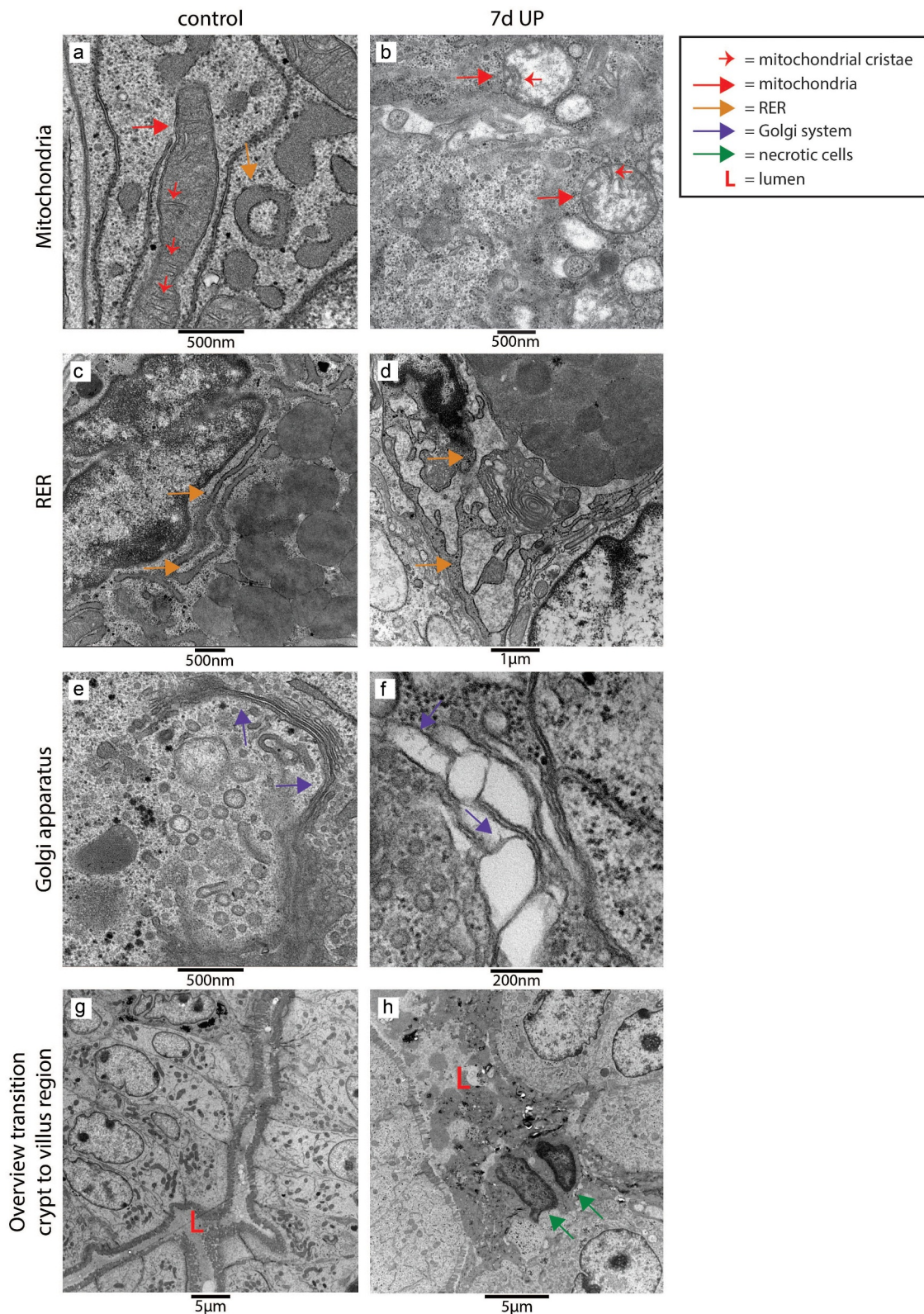


Figure 4. Organelle and cellular morphology of secretory cells (goblet cells and Paneth cells) in the crypt to villus transition region in the distal ileum of premature lambs imaged with TEM. In control animals, mitochondria (**A**; red arrows, cristae indicated by small red arrows), RER (**C**; orange arrows) and Golgi apparatus (**E**; purple arrows) of secretory cells had a structurally normal appearance. In IA UP exposed animals, these organelles were morphologically disrupted (**B**, **D**, **F**). In addition, cells with necrotic characteristics (green arrows) were observed in the lumen (L) of IA UP exposed animals (h), but not in controls (g). Abbreviations: IA: intra-amniotic, L: lumen, RER: rough endoplasmic reticulum, TEM: transmission electron microscopy, UP: *Ureaplasma Parvum*.

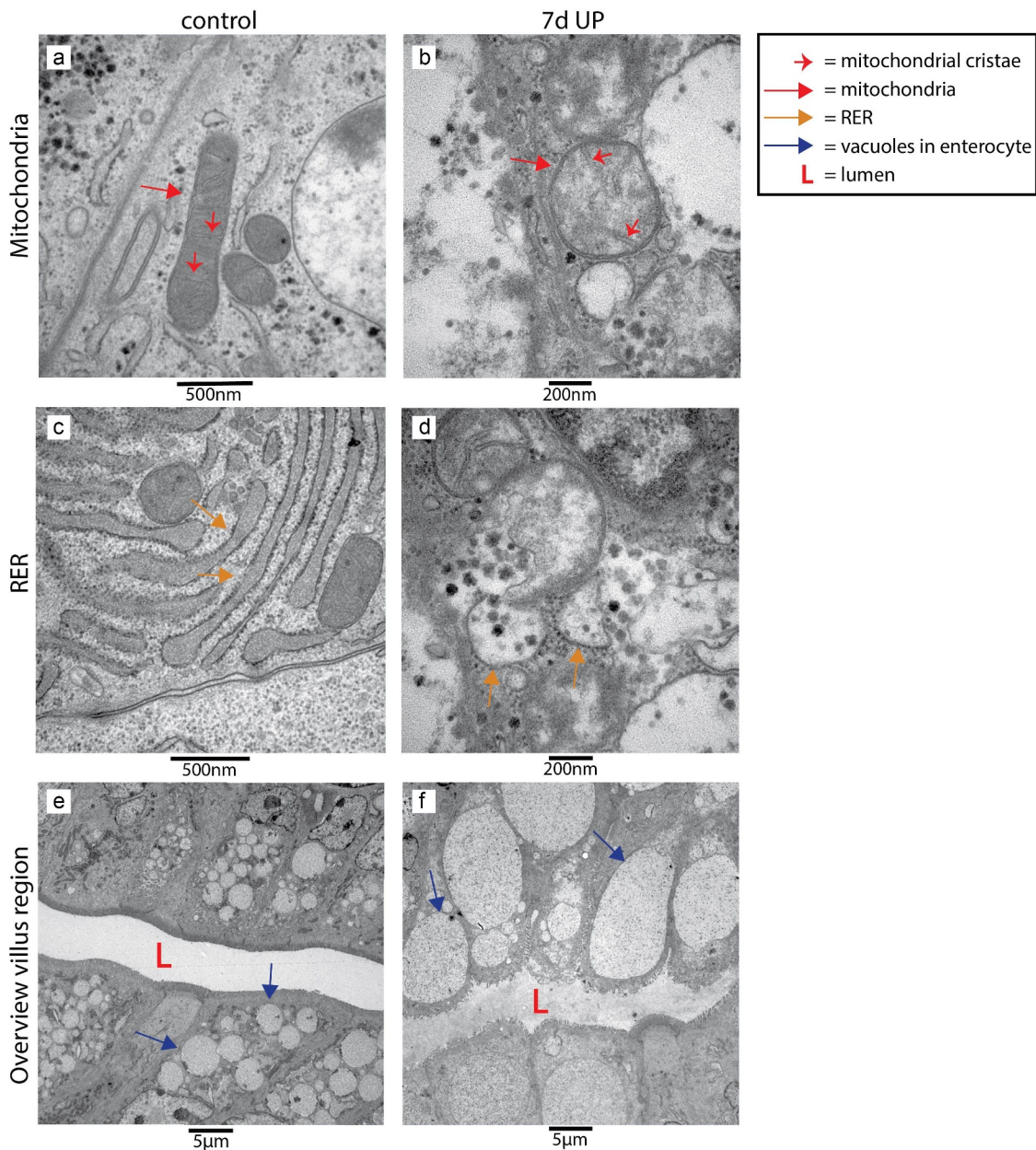


Figure 5. Organelle and cellular morphology of enterocytes in the villus region in the distal ileum of premature lambs imaged with TEM. Mitochondria (A; red arrows, mitochondrial cristae indicated by small red arrows) and RER (C; orange arrows) of enterocytes were normal in control animals. In IA UP exposed animals these organelles were morphologically disrupted (b, d). In addition, enterocytes containing small vacuoles (blue arrows) were observed in control animals (e), whereas larger vacuoles were detected in IA UP exposed lambs (f). Abbreviations: IA: intra-amniotic, L: lumen, RER: rough endoplasmic reticulum, TEM: transmission electron microscopy, UP: *Ureaplasma Parvum*.

Villi were largely necrotic in ileal NEC samples. Comparable to the findings in IA UP exposed animals, mitochondria and RER of enterocytes, but also goblet cells, were morphologically disrupted in all the remaining villi of NEC patients (Figure 6j), whereas a normal

organelle appearance was observed in control samples (Figure 6i).

Collectively, there is remarkable overlap between the cellular morphological alterations observed in the ileum of NEC patients and those observed in the ovine terminal ileum following IA UP exposure.

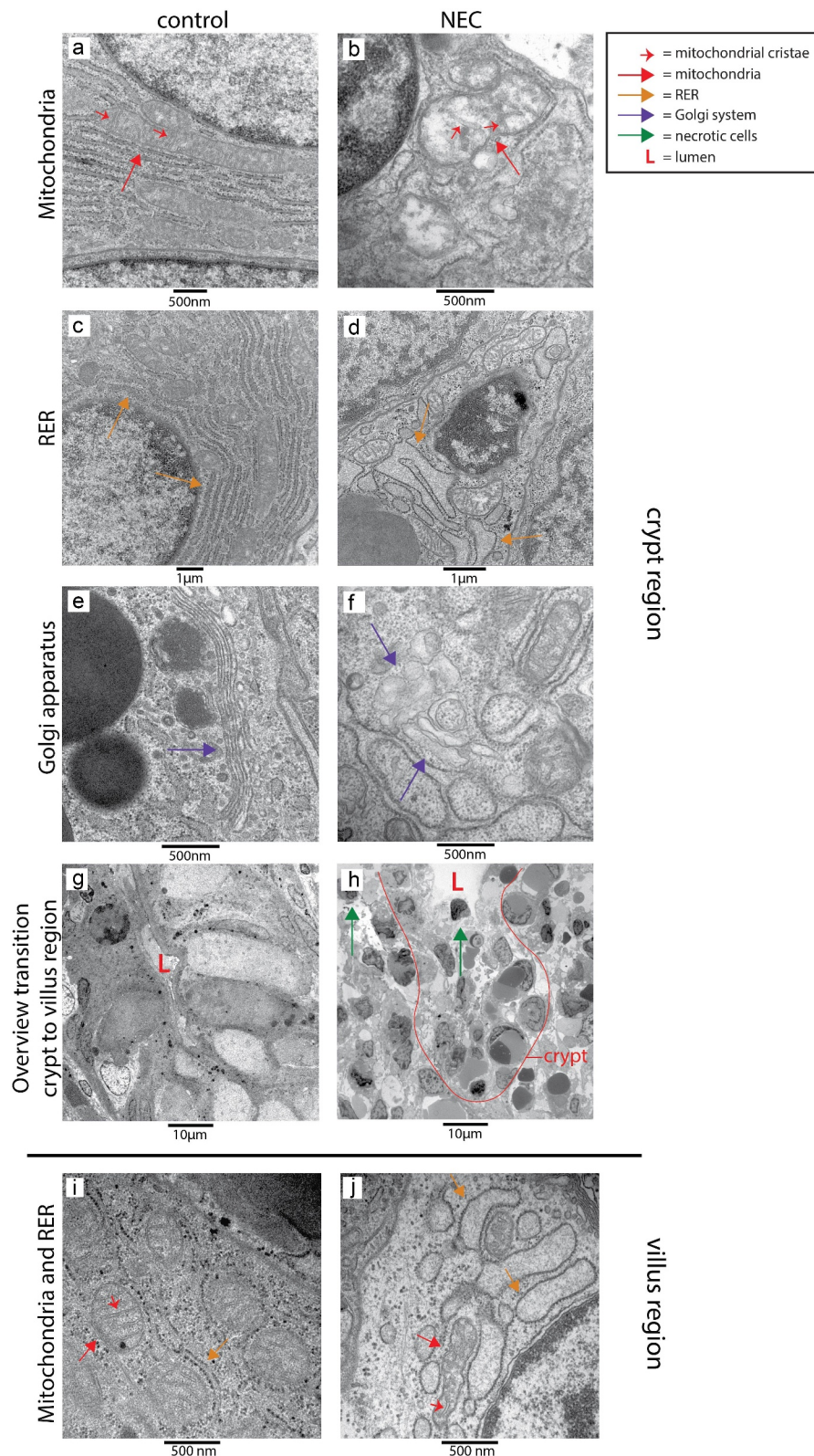


Figure 6. Organelle and cellular morphology of enterocytes and secretory cells (goblet cells and Paneth cells) in the ileal crypt region and villus region of NEC patients and controls detected with TEM. Mitochondria (red arrows; mitochondrial cristae indicated by small red arrows), RER (orange arrows) and the Golgi apparatus (purple arrows) of epithelial and secretory cells were normal in the crypt region of control infants (**A, C, E**), but morphologically disrupted in the NEC patients (**B, D, F**). Interestingly, compared to control ileal samples (**g**), large amounts of intestinal cells with necrotic characteristics (green arrows) were present in the crypts of NEC patients (**h**). Similarly, mitochondria (red arrows, mitochondrial cristae are indicated by small red arrows) and RER (orange arrows) appeared normal in goblet cells and enterocytes in the ileum of control infants (**i**), whereas these organelles were morphologically disrupted in goblet cells and enterocytes in the ileum from NEC patients (**j**). Abbreviations: L: lumen, NEC: necrotizing enterocolitis, RER: rough endoplasmic reticulum, TEM: transmission electron microscopy.

Discussion

Key findings of the current study are increased numbers of goblet cells and increased mucus layer thickness, which may be caused by mucus hypersecretion, in the distal ileum of premature lambs following UP-induced chorioamnionitis, demonstrating that mucus barrier alterations occur in response to a microbial trigger already *in utero*. These mucus barrier alterations were associated with pro-apoptotic intestinal epithelial ER stress and cellular morphological disruptions that largely overlap with the observations in the ileum of NEC patients. This indicates that, although the increased mucus layer thickness at the short term could be favorable, antenatal UP exposure likely poses a large burden on the resilience of goblet cells and therefore may predispose to detrimental outcomes of the premature ileum.

Although, at the time point of premature delivery, no gut injury (villus atrophy) and alterations in intestinal epithelial proliferation were detected and no increase of intestinal epithelial cell death (CC3) was observed in the majority of UP exposed animals, UP exposure caused considerable disruptions at cellular level. Interestingly, pro-apoptotic ER stress, which probably results from mucus hypersecretion, seems to be an important mechanism contributing to hampered goblet cell resilience. CHOP-positive cell counts were increased following IA UP exposure and the observed cellular morphological alterations are indicative of ER stress. Moreover, pro-apoptotic intestinal epithelial ER stress was previously observed at a later time point in the course of LPS-induced chorioamnionitis and was then paralleled by reduced goblet cell numbers.¹⁴ Together, these findings support the idea that UP is not just an innocent bystander during chorioamnionitis but contributes to its pathophysiology.¹ One might argue that the fact that the increased CHOP immunoreactivity was not accompanied by altered BiP expression at the studied time point contradicts the involvement of ER stress. However, in an earlier study in fetal sheep we observed that BiP and CHOP immunoreactivity did not peak at the same moment following intra-uterine inflammation.¹⁴ Of note, overt organelle disruptions of both crypt and villi were only detected in 4 out of 6 UP exposed animals studied by TEM and there was also pronounced variability in other studied

parameters. This reflects the variable phenotype of infants prenatally exposed to UP in the clinical setting,²⁹ which to date is not fully understood, but has been associated with the magnitude of the host response.³⁰

The clinical relevance of the antenatal findings in our translational model is substantiated by comparable findings in clinical biopsies from NEC patients. In ileal samples from patients with NEC, morphological alterations on organelle level (as assessed by TEM analysis) that were observed in secretory cells of the intestinal crypts largely overlapped with our findings in UP-induced chorioamnionitis (morphologically disrupted RER and mitochondria). In clinical NEC tissues however, these changes were present in all crypt-villus axes and extended to the whole crypt instead of predominantly in the transition region from crypt to villus. This could be related to the more severe nature of NEC, its multifactorial origin, including the influence of the microbiome and exposure to enteral nutrition, and the longer duration of pro-inflammatory insults when compared to our antenatal pre-clinical setting. Importantly, even temporal disturbance of resilience of intestinal goblet cells could predispose the vulnerable infant to injury following additional pro-inflammatory hits, such as sepsis³¹ and mechanical ventilation,³² and may in part explain the association between chorioamnionitis and postnatal development of NEC.

Increased mucus layer thickness is likely caused by an increased secretion of mucus by goblet cells. Alternatively, other factors, such as increased ion secretion or altered mucus proteolysis, could be involved in the increased mucus layer thickness following IA UP exposure.^{33,34}

UP-induced inflammation could underlie the increased number of mature goblet cells and the postulated increased mucus secretion rate, as several pro-inflammatory cytokines have been reported to induce mucus secretion.³⁵ Consistently, (mild) inflammation was detected at the time point of delivery in this study and we have previously shown intestinal inflammation in comparable ovine studies.^{5,21} Moreover, direct contact between UP and intestinal goblet cells could trigger mucus release via UP-induced activation of Toll-like receptors (TLRs).³⁶ In the mouse colon,

sentinel goblet cells have been described at the entrance of intestinal crypts that secrete MUC2 upon endocytosis of a TLR2/1 ligand and that subsequently also promote mucus release from adjacent reactive goblet cells.³⁷ In addition, UP might have a negative on the GI tract by altering the pH of the amniotic fluid and the intestinal mucus layer because of its effects on ammonia and urease metabolism.³⁸

Interestingly, several findings support the concept that the thicker mucus layer observed in the distal ileum may result from a similar mechanism. First, goblet cells present in the transition region from crypt to villus display a cellular morphology (observed with TEM) of ER stress (disrupted RER and Golgi apparatus) and oxidative stress (disrupted mitochondria), whereas this phenotype is less pronounced in goblet cells in the villus region. These observations are considered to be causally linked to the postulated increased mucin production, as mucins are processed by the ER and the Golgi apparatus and ER stress and oxidative stress can give rise to a vicious cycle.^{20,39} Reactive oxygen species (ROS) can disturb ER protein folding and ER stress can increase ROS formation directly through oxidative protein folding in the ER and indirectly through mitochondrial uptake of Ca^{2+} released from the ER.³⁹ Second, in the transition region from crypt to villus, cells with necrotic characteristics were observed that may represent sentinel goblet cells that were expelled into the intestinal lumen following mass mucus secretion.^{37,40}

Interestingly, cellular changes (as assessed by TEM analysis) and increased pro-apoptotic levels of ER stress (CHOP) were also detected in intestinal villi, suggesting that, besides goblet cells, enterocytes are affected by intrauterine inflammation. In control animals, vacuolated enterocytes were observed, which is a hallmark of fetal enterocytes that results from amniotic fluid macromolecule uptake.²⁸ In UP exposed animals however, these vacuoles were much larger. Although the precise nature of this observation remains to be elucidated, similar findings were described in a murine NEC model.⁴¹ That study suggested that these vacuoles were giant lysosomes resulting from lysosomal overloading due to excessive endocytosis and

autophagy and these structures were implicated to be involved in NEC pathophysiology.⁴¹ In addition, we observed morphologically disrupted organelles (RER and mitochondria) in vacuolated enterocytes as well, indicating elevated levels of ER stress in the villus region. Whether this ER stress is causally related to the presence of larger vacuoles is an interesting topic for future research.

Regardless of the high translation value of the research findings from large animal studies, an inherent limitation of the current study is the relatively low animal numbers per treatment group. Unfortunately, this is an unavoidable drawback of preclinical large animal models.

Of note, the mucus thickness alteration observed in the current study is the first indication that goblet cell alterations have a big impact on their mucus secretory behavior. These functional consequences and postulated underlying mechanisms need to be confirmed and extended in ongoing follow-up studies.

In conclusion, UP-induced chorioamnionitis increased the number of goblet cells, which may be related to an increased mucus secretion rate and the observed increased ileal mucus layer thickness. It is likely these changes take place at the expense of goblet cell resilience, as they were associated with pro-apoptotic intestinal epithelial ER stress and the cellular morphological disruptions largely overlapped with the observations of the ileum from NEC patients. Interestingly, intrauterine inflammation also negatively affected enterocytes. Even temporal disruption of intestinal goblet cell and enterocyte resilience could predispose the vulnerable infant to injury following additional pro-inflammatory hits and may in part explain the association between chorioamnionitis and NEC. Therefore, timely initiation of interventions that may support intestinal recovery after chorioamnionitis, such as enteral feeding intervention,⁴² could aid in preserving a healthy mucus barrier and preventing NEC development.

Acknowledgments

The authors would like to thank Ruben Visschers, Hamit Cakir and Olivier Theeuws for their help with collecting human intestinal samples and Nico Kloosterboer for his excellent technical support. In addition, we also would like to thank

Elly van Donselaar for her insight in the TEM methodology and Hans Duimel and the other members of the microscopy CORE laboratory at FHML for their support in the TEM work.

Authors contribution statement:

Conceptualization: CG, MH, TW.; methodology: CG, IL, CLI, KM, LK, GB, WW, TW; software: CG, KM; validation: CG, IL, KM, LK, TW; formal analysis: CG, IL, KM, LK; investigation: CG, IL, CLI, KM, LK, OS, GB, WG, LZ, TW; resources: MH, BK, WG, LZ, TW; data curation: CG, IL, KM; writing original article: CG, IL, TW; writing—review and editing: MH, CLI, LK, BW, WW, OS, GB, WG, LZ; visualization: CG, IL, KM; supervision: TW; project administration: MH, CG, KM; funding acquisition, MH, LZ, TW. All authors have read and agreed to the published version of the manuscript.

Disclosure statement

No potential conflict of interest was reported by the authors.

Funding

This work was financially supported by the ‘Kinderonderzoeksfonds Limburg’, (TW), NUTRIM: School of Nutrition and Translational Research in Metabolism and the NUTRIM graduate programme (IL). Data availability statement: The data presented in this study are available in this article and in the Supplementary Materials.

ORCID

Tim GAM Wolfs  <http://orcid.org/0000-0003-4417-4144>

Ethics approval statement:

Animal experiments were approved by the animal experimentation committee of Maastricht University (registration number PV2015–005–02). The human part of this study was approved by the Medical Ethical Committee of Maastricht University Medical Centre (registration number 1–5–185). All parents gave written informed consent.

References

1. Sweeney EL, Dando SJ, Kallapur SG, Knox CL. The human ureaplasma species as causative agents of chorioamnionitis. *Clin Microbiol Rev.* 2017;30(1):349–379. doi:10.1128/CMR.00091-16.
2. Thomas W, Speer CP. Chorioamnionitis: important risk factor or innocent bystander for neonatal outcome? *Neonatology.* 2011;99(3):177–187. doi:10.1159/000320170.
3. Gantert M, Been JV, Gavilanes AW, Garnier Y, Zimmermann LJI, Kramer BW. Chorioamnionitis: a multiorgan disease of the fetus? *J Perinatol: Offl J California Perinatal Ass.* 2010;30Suppl(S1):S21–30. doi:10.1038/jp.2010.96.
4. Heymans C, de Lange IH, Hütten MC, Lenaerts K, de Ruijter NJE, Kessels LCGA, Rademakers G, Melotte V, Boesmans W, Saito M, *et al.* Chronic intra-uterine ureaplasma parvum infection induces injury of the enteric nervous system in ovine fetuses. *Front Immunol.* 2020;11:189. doi:10.3389/fimmu.2020.00189.
5. Wolfs TG, Kallapur SG, Knox CL, Thuijls G, Nitsos I, Polglase GR, Collins JJP, Kroon E, Spierings J, Shroyer NF, *et al.* Antenatal ureaplasma infection impairs development of the fetal ovine gut in an IL-1-dependent manner. *Mucosal Immunol.* 2013;6(3):547–556. doi:10.1038/mi.2012.97.
6. Gotsch F, Romero R, Kusanovic JP, MAZAKI-TOVI S, Pineles BL, Erez O, Espinoza J, Hassan SS. The fetal inflammatory response syndrome. *Clin Obstet Gynecol.* 2007;50(3):652–683. doi:10.1097/GRF.0b013e31811ebef6.
7. Sprong KE, Mabenge M, Wright CA, Govender S. Ureaplasma species and preterm birth: current perspectives. *Crit Rev Microbiol.* 2020;46(2):169–181. doi:10.1080/1040841X.2020.1736986.
8. Been JV, Lievens S, Zimmermann LJ, Kramer BW, Wolfs TGAM. Chorioamnionitis as a risk factor for necrotizing enterocolitis: a systematic review and meta-analysis. *J Pediatr.* 2013;162(2):236–242.e232. doi:10.1016/j.jpeds.2012.07.012.
9. Neu J, Walker WA. Necrotizing enterocolitis. *N Engl J Med.* 2011;364(3):255–264. doi:10.1056/NEJMra1005408.
10. Halpern MD, Denning PW. The role of intestinal epithelial barrier function in the development of NEC. *Tissue Barriers.* 2015;3(1–2):e1000707. doi:10.1080/21688370.2014.1000707.
11. McElroy SJ, Prince LS, Weitkamp JH, Reese J, Slaughter JC, Polk DB. Tumor necrosis factor receptor 1-dependent depletion of mucus in immature small intestine: a potential role in neonatal necrotizing enterocolitis. *Am J Physiol Gastrointest Liver Physiol.* 2011;301(4):G656–666. doi:10.1152/ajpgi.00550.2010.
12. Schaart MW, de Bruijn AC, Bouwman DM, de Krijger RR, van Goudoever JB, Tibboel D, Renes IB. Epithelial functions of the residual bowel after surgery for necrotising enterocolitis in human infants. *J Pediatr Gastroenterol Nutr.* 2009;49(1):31–41. doi:10.1097/MPG.0b013e318186d341.
13. Elgin TG, Fricke EM, Gong H, Reese J, Mills DA, Kalantera KM, Underwood MA, McElroy SJ. Fetal exposure to maternal inflammation interrupts murine intestinal development and increases susceptibility to neonatal intestinal injury. *Dis Model Mech.* 2019, 21 October;12(10). doi:10.1242/dmm.040808.

14. van Gorp C, de Lange IH, Massy KRI, Kessels L, Jobe AH, Cleutjens JPM, Kemp MW, Saito M, Usada H, Newnham J, *et al.* Intestinal goblet cell loss during chorioamnionitis in fetal lambs: mechanistic insights and postnatal implications. *Int J Mol Sci.* 2021;22(4):1946. doi:10.3390/ijms22041946.
15. Coleman OI, Haller D. ER stress and the UPR in shaping intestinal tissue homeostasis and immunity. *Front Immunol.* 2019;10:2825. doi:10.3389/fimmu.2019.02825.
16. Afrazi A, Branca MF, Sodhi CP, Good M, Yamaguchi Y, Egan CE, Lu P, Jia H, Shaffiey S, Lin J, *et al.* Toll-like receptor 4-mediated endoplasmic reticulum stress in intestinal crypts induces necrotizing enterocolitis. *J Biol Chem.* 2014;289(14):9584–9599. doi:10.1074/jbc.M113.526517.
17. Lu P, Struijs MC, Mei J, Witte-Bouma J, Korteland-van Male AM, de Bruijn ACJM, van Goudoever JB, Renes IB. Endoplasmic reticulum stress, unfolded protein response and altered T cell differentiation in necrotizing enterocolitis. *PloS one.* 2013;8(10):e78491. doi:10.1371/journal.pone.0078491.
18. Hetz C. The unfolded protein response: controlling cell fate decisions under ER stress and beyond. *Nat Rev Mol Cell Biol.* 2012;13(2):89–102. doi:10.1038/nrm3270.
19. Ron D, Walter P. Signal integration in the endoplasmic reticulum unfolded protein response. *Nat Rev Mol Cell Biol.* 2007;8(7):519–529. doi:10.1038/nrm2199.
20. McGuckin MA, Eri RD, Das I, Lourie R, Florin TH. ER stress and the unfolded protein response in intestinal inflammation. *Am J Physiol Gastrointest Liver Physiol.* 2010;298(6):G820–832. doi:10.1152/ajpgi.00063.2010.
21. van Gorp C, de Lange IH, Spiller OB, Dewez F, Cillero Pastor B, Heeren RMA, Kessels L, Kloosterboer N, van Gemert WG, Beeton ML, *et al.* Protection of the ovine fetal gut against ureaplasma-induced chorioamnionitis: a potential role for plant sterols. *Nutrients.* 2019;11(5):968. doi:10.3390/nu11050968.
22. Hurd EA, Holmén JM, Hansson GC, Domino SE. Gastrointestinal mucins of Fut2-null mice lack terminal fucosylation without affecting colonization by *Candida albicans*. *Glycobiology.* 2005;15(10):1002–1007. doi:10.1093/glycob/cwi089.
23. Yamabayashi S. Periodic acid-Schiff-alcian blue: a method for the differential staining of glycoproteins. *Histochem J.* 1987;19(10–11):565–571. doi:10.1007/BF01687364.
24. Bankhead P, Loughrey MB, Fernández JA, Dombrowski Y, McArt DG, Dunne PD, McQuaid S, Gray RT, Murray LJ, Coleman HG, *et al.* QuPath: open source software for digital pathology image analysis. *Sci Rep.* 2017;7(1):16878. doi:10.1038/s41598-017-17204-5.
25. Gustafsson JK, Ermund A, Johansson MEV, Schütte A, Hansson GC, Sjövall H. An ex vivo method for studying mucus formation, properties, and thickness in human colonic biopsies and mouse small and large intestinal explants. *Am J Physiol Gastrointest Liver Physiol.* 2012;302(4):G430–G438. doi:10.1152/ajpgi.00405.2011.
26. Gussenhoven R, Westerlaken RJJ, Ophelders DRMG, Jobe AH, Kemp MW, Kallapur SG, Zimmermann LJ, Sangild PT, Pankratova S, Gressens P, *et al.* Chorioamnionitis, neuroinflammation, and injury: timing is key in the preterm ovine fetus. *J Neuroinflammation.* 2018;15(1):113. doi:10.1186/s12974-018-1149-x.
27. Hasnain SZ, Evans CM, Roy M, Gallagher AL, Kindrachuk KN, Barron L, Dickey BF, Wilson MS, Wynn TA, Grecis RK, *et al.* Muc5ac: a critical component mediating the rejection of enteric nematodes. *J Exp Med.* 2011;208(5):893–900. doi:10.1084/jem.20102057.
28. Skrzypek T, Szymańczyk S, Ferenc K, Kazimierczak W, Szczepaniak K, Zabielski R. The contribution of vacuolated foetal-type enterocytes in the process of maturation of the small intestine in piglets. Invited review. *J Anim Feed Sci.* 2018;27(3):187–201. doi:10.22358/jafs/94167/2018.
29. Waites KB, Katz B, Schelonka RL. Mycoplasmas and ureaplasmas as neonatal pathogens. *Clin Microbiol Rev.* 2005;18(4):757–789. doi:10.1128/CMR.18.4.757-789.2005.
30. Sweeney EL, Dando SJ, Kallapur SG, Knox CL. The human ureaplasma species as causative agents of chorioamnionitis. *Clin Microbiol Rev.* 2016;30:349–379.
31. Machado JR, Soave DF, da Silva MV, de Menezes LB, Etchebere RM, Monteiro MLGDR, Dos Reis MA, Corrêa RRM, Celes MRN. Neonatal sepsis and inflammatory mediators. *Mediators Inflamm.* 2014;2014:269681. doi:10.1155/2014/269681.
32. Bose CL, Laughon MM, Allred EN, Michael O’Shea T, Van Marter LJ, Ehrenkranz RA, Fichorova RN, Leviton A. Systemic inflammation associated with mechanical ventilation among extremely preterm infants. *Cytokine.* 2013;61(1):315–322. doi:10.1016/j.cyto.2012.10.014.
33. Gustafsson JK, Ermund A, Ambort D, Johansson MEV, Nilsson HE, Thorell K, Hebert H, Sjövall H, Hansson GC. Bicarbonate and functional CFTR channel are required for proper mucin secretion and link cystic fibrosis with its mucus phenotype. *J Exp Med.* 2012;209(7):1263–1272. doi:10.1084/jem.20120562.
34. Nyström EEL, Birchenough GMH, van der Post S, Arike L, Gruber AD, Hansson GC, Johansson MEV. Calcium-activated chloride channel regulator 1 (CLCA1) Controls mucus expansion in colon by proteolytic activity. *EBioMedicine.* 2018;33:134–143. doi:10.1016/j.ebiom.2018.05.031.
35. Cornick S, Tawiah A, Chadee K. Roles and regulation of the mucus barrier in the gut. *Tissue Barriers.* 2015;3(1–2):e982426. doi:10.4161/21688370.2014.982426.
36. Triantafilou M, De Glanville B, Aboklaish AF, Spiller OB, Kotecha S, Triantafilou K. Synergic activation of toll-like receptor (TLR) 2/6 and 9 in response to

- Ureaplasma parvum & urealyticum in human amniotic epithelial cells. *PloS one*. 2013;8(4):e61199. doi:10.1371/journal.pone.0061199.
37. Birchenough GM, Nyström EE, Johansson ME, Hansson GC. A sentinel goblet cell guards the colonic crypt by triggering Nlrp6-dependent Muc2 secretion. *Sci*. 2016;352(6293):1535–1542. doi:10.1126/science.aaf7419.
 38. Kallapur SG, Kramer BW, Jobe AH. Ureaplasma and BPD. *Semin Perinatol*. 2013;37(2):94–101. doi:10.1053/j.semperi.2013.01.005.
 39. Cao SS, Kaufman RJ. Endoplasmic reticulum stress and oxidative stress in cell fate decision and human disease. *Antioxid Redox Signal*. 2014;21(3):396–413. doi:10.1089/ars.2014.5851.
 40. Zhang M, Wu C. The relationship between intestinal goblet cells and the immune response. *Biosci Rep*. 2020;40(10). doi:10.1042/BSR20201471.
 41. Yamoto M, Alganabi M, Chusilp S, Lee D, Yazaki Y, Lee C, Li B, Pierro A. Lysosomal overloading and necrotizing enterocolitis. *Pediatr Surg Int*. 2020;36(10):1157–1165. doi:10.1007/s00383-020-04724-x.
 42. de Lange IH, van Gorp C, Eeftinck Schattenkerk LD, van Gemert WG, Derikx JPM, Wolfs TGAM. Enteral feeding interventions in the prevention of necrotizing enterocolitis: a systematic review of experimental and clinical studies. *Nutrients*. 2021;13(5):1726. doi:10.3390/nu13051726.